EUROPEAN COMMISSION
DIRECTORATE-GENERAL
Joint Research Centre

Institute for Reference Materials and Measurements

Determination by Isotope Ratio Mass Spectrometry of the absolute isotope amount fractions of oxygen and nitrogen in Nitrous Oxide.

Mihai Varlam,Staf Valkiers, Michael Berglund, PhilipTaylor
Institute for Reference Materials and Measurements, JRC-European Commission, B-2440 Geel, Belgium.

Report EUR 22677 EN

The mission of IRMM is to promote a common and reliable European measurement system in support of EU policies.

European Commission
Directorate-General Joint Research Centre
Institute for Reference Materials and Measurements

Contact information
S. Valkiers
European Commission
Directorate-General Joint Research Centre
Institute for Reference Materials and Measurements
Retieseweg 111
B-2440 Geel • Belgium

E-mail: staf.valkiers@ec.europa.eu

Tel.: +32 (0)14 571 639
Fax: +32 (0)14 571 863

http://www.irmm.jrc.be
http://www.jrc.ec.europa.eu

EUR Report 22677 EN
ISSN 1018-5593
Luxembourg: Office for Official Publications of the European Communities

ISBN 978-92-79-03347-6

Printed in Belgium

EUROPEAN COMMISSION
DIRECTORATE-GENERAL
Joint Research Centre

Institute for Reference Materials and Measurements

Determination by Isotope Ratio Mass Spectrometry of the absolute isotope amount fractions of oxygen and nitrogen in Nitrous Oxide.

Mihai Varlam,Staf Valkiers, Michael Berglund, PhilipTaylor
Institute for Reference Materials and Measurements, JRC-European Commission, B-2440 Geel, Belgium.

European Commission

EUR 22677 EN – DG Joint Research Centre, Institute for Reference Materials and Measurements –IRMM-IM
Luxembourg: Office for Official Publications of the European Communities
2007 – 27 pp. – 21 x 30 cm
Scientific and Technical Research series
ISBN 978-92-79-03347-6

Abstract

The significant interest related to atmospheric Nitrous oxide as a greenhouse gas and as a tool to regulate the Ozone concentration is well-known and requires to define a precise budget in the atmosphere for this gas. Therefore, the isotopic measurements are proposed to become the necessary additional instrument to better quantify this budget. The lack of a real comparability tool for the disparate Nitrous oxide isotopic measurement done required to start the work related to the development of a Reference material for Nitrogen and Oxygen in this gas.

A measurement procedure for the complete isotope characterization of atmospheric Nitrous oxide sample has been developed and applied to establish a first Reference material for this gas. The whole work has been based on the peculiar instrumental capabilities of "Avogadro" MAT 271IRMS. Additional hardware and software improvement has been done for this mass spectrometer to apply the proposed method.

Introduction

The special significance of atmospheric N_2O for the global environment finds its origin in two distinct properties. Foremost is that N_2O regulates stratospheric ozone. This is the consequence of its reaction in the stratosphere with $O(^1D)$ radicals according to $O(^1D) + N_2O \rightarrow 2\ NO$ or $N_2 + O_2$. The reaction path to NO, which occurs for about 60% constitutes the dominant source of stratospheric NO that participates to catalytic reactions which destroy ozone. Therefore, N_2O affects a number of stratospheric properties and more important, indirectly regulates the amount of ultraviolet radiation reaching the earth surface.

The second important attribute is that N_2O is a potent greenhouse gas due to its strong absorption in several infrared bands in the 7.7 to 17 μm range, its long atmospheric chemical life-time of around 130 years and its significant atmospheric mixing ratio of about 315 nanomole/ mole.

Nitrous oxide is a trace gas that is produced especially during microbial energy exchange reactions involving both reduced $(NH_3)^+$ and oxidized $(NO_3)^-$ forms of nitrogen. The major sources are oceans and soils, both being extensive and complex. This coupled with its long atmospheric residence time will lead to small gradients and associated problems in assessing the various source strengths.

The last measurements indicate a current tropospheric concentration of about 313 ppbv and an increasing at a rate of ~0,25% per year has been observed which produced a real concern for the atmospheric research community. Estimates of the natural sources of N_2O range from 1.4 to 5.2 Tg N/year for oceanic sources and 2.7 to 7.7 Tg N/year from tropical and temperate soils. The observed atmospheric increase is considered to arise primarily from application of fertilizers to cultivated soils, but animal waste, biomass burning, fuel combustion and industrial processes

also contribute. Practically, the knowledge about individual source strengths is poor and lacks experimental verification.

Generally, the stable isotopic composition of atmospheric trace gases provides valuable additional information about their origin and fate that cannot be determined only from concentration measurements. Biological source and loss processes, such as bacterial production of methane or photosynthetic consumption of CO_2, are typically accompanied by isotopic selectivity associated with the kinetics of bond formation and destruction.

In an effort to reduce the errors in these estimates and balance the N_2O budget, investigation of the stable isotopic signatures of the various sources and sinks have been carried out by several research groups.

It must be emphases that, of the most three important biologically mediated greenhouse gases the understanding of the isotopic budget of nitrous oxide lags far behind that of carbon dioxide and methane. This is due to problems inherent in collection and analytical techniques which hamper the ability to make measurements of very high precision. It is also due to the fact that a limited database and a wide range of used reference materials for Nitrogen and Oxygen associated to various analytical measurement techniques has made difficult to assign a unique value to each source and sink terms. Moreover, the theoretical studies show that since photolysis is the most important sink in the atmospheric nitrous oxide, the photolytic isotopic fractionation must be taken into account when constructing a global N_2O budget. Also, fractionation associated with the minor sink, reaction with excited atomic oxygen must be taken into account. The fractionation due to this reaction has been determined for the oxygen species, ^{17}O and ^{18}O, and has been shown to be mass dependent with -6±1. Finally it must be noted that the asymmetry of the N_2O molecule presents a unique opportunity to investigate an additional set of parameters with which N_2O budget could be constructed. The fractionation for the two ^{15}N isotopomers is predicted to be significantly different according to the theory of Yung & Miller. Also, the scientific community is waiting for the right results which will prove or not if the biologically mediated source terms have unique ^{15}N position signatures as well.

Taking into consideration the real need for developing a real isotopic budget for atmospheric N_2O and related to that, bearing in mind the necessity for a Reference Material in the gas form for both Nitrogen and Oxygen, the work proposed to elaborate an adequate Isotope Ratio measurement procedure, based only on fundamental assumption. Avoiding questionable separation techniques, this new procedure was applied for direct measurement of atmospheric Nitrous oxide samples. The research has been directed into two distinct working field – developing and implementing new instrumental facilities for “Avogadro” MAT 271 – IRMS in order to extend the range of isotope ratio measurements and to elaborate the measurement method which has been afterwards applied to establish a first gaseous reference material.

1. Analytical topic

Practically there are twelve N_2O isotopomers (table 1) but only five species are of interest when analyzing N_2O isotopes: the abundant isotopomer $^{14}N^{14}N^{16}O$ and the rare isotopomers $^{14}N^{15}N^{16}O$, $^{15}N^{14}N^{16}O$, $^{14}N^{14}N^{17}O$ and $^{14}N^{14}N^{18}O$. The two ^{15}N species are indistinguishable with current mass spectrometric techniques. Also, the two rare oxygen species have in the past been assumed to be mass-dependently related although it has recently been shown that there is a slight mass-independent enrichment of ^{17}O in troposheric N_2O samples which is as yet unaccounted for.

As the two N atoms in the linear N_2O molecule are not equivalent (figure 1), from the isotopic ratio measurements point of view, a distinction is usually made between the δ value of the terminal N atom in N_2O (designated in the following by $^{1}\delta^{15}N$) , the middle N ($^{2}\square^{15}N$) and the average of both ($\delta^{15}N$). Likewise the isotope ratios will be designated $^{15}R_1$ and $^{15}R_2$.

Table 1

Isotopomer	mass	Natural abundance (ppm)	Share/% Species with same m
$^{14}N^{14}N^{16}O$	44	990143.61	100.00
$^{14}N^{14}N^{17}O$	45	385.76	4.98
$^{14}N^{15}N^{16}O$	45	3642.65	47.04
$^{15}N^{14}N^{16}O$	45	3716.00	47.98
$^{14}N^{14}N^{18}O$	46	2079.94	99.21
$^{14}N^{15}N^{17}O$	46	1.42	0.07
$^{15}N^{14}N^{17}O$	46	1.45	0.07
$^{15}N^{15}N^{16}O$	46	13.67	0.65
$^{14}N^{15}N^{18}O$	47	7.65	49.48
$^{15}N^{14}N^{18}O$	47	7.81	50.48
$^{15}N^{15}N^{17}O$	47	< 0.001	0.03
$^{15}N^{15}N^{18}O$	48	0.03	100.00

Because the isotopomers of interest are isobaric with those of CO_2 (masses 44, 45 and 46) and since CO_2 in natural environment is generally ~1000 times more abundant, the methods used for isotopic analysis employed until now techniques, which involve selective decomposition of N_2O and subsequent analysis of products. For this reason, the isotopic reference materials for N_2O have been atmospheric N_2 for ^{15}N and SMOW-*Standard Mean Ocean Water* for oxygen isotopes.

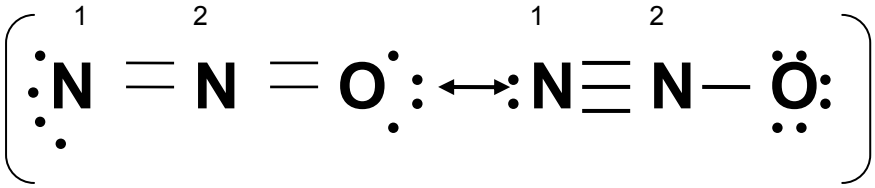

Fig.1.: Mesomeric forms of N_2O in resonance with each other. 1 and 2 indicate the position-dependent ^{15}N designation

Also must be emphases that all the studies reported related to the conversion from molecular to elemental isotope ratios do not deal with the position-dependent ^{15}N enrichment or assume from the outset a complete statistical isotope distribution, which introduces potential biases for the measured values.

Taking into account the large number of existing isotopomers and due to limitation of sensibility for the usual isotope ratio mass spectrometer, the elemental isotope ratios cannot be derived from the measurements of ^{45}R and ^{46}R alone, without any further assumptions.

The main target of this project was therefore to establish correct isotope ratio measurements in gaseous N_2O in order to calculate, without additional doubtful assumptions, the elemental isotope ratios for nitrogen – $^{15}R_1$ and $^{15}R_2$ and for Oxygen – ^{17}R and ^{18}R. The origin of the whole measurement procedure developed

was the striking unique capabilities of MAT 271 –IRMS to perform “absolute” isotope ratios measurements based only on the gas flow characteristics from the special designed inlet system.

The first tests were intended to investigate the basics of the ionization-fragmentation processes in the mass spectrometer electron impact ion source for a N_2O gas input. A typical N_2O mass spectrometric cracking pattern is shown in figure 2.

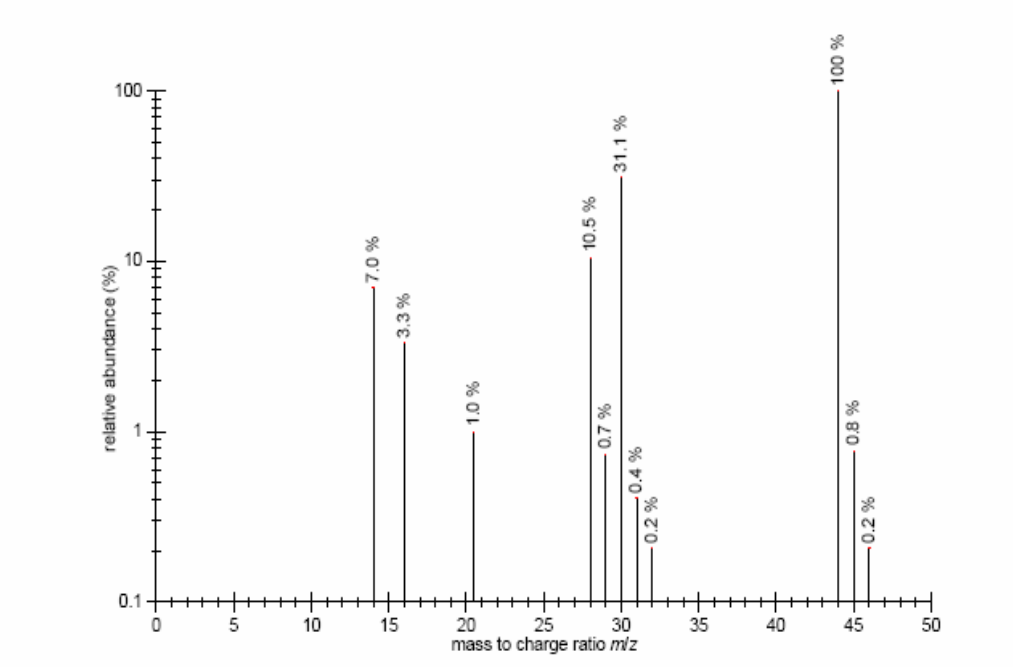

Figure 2.: Typical mass spectrum of N_2O

The mass spectrum shown above is the result of these processes in the ion source, which could be basically described as fragmentation and recombination reactions. A short summary of these potential processes that are happening when N_2O gas flow is entering in the electron impact ion source are described bellow:

Ionization and fragmentation reactions:

$$N_2O + e \rightarrow N_2O^+(mass \quad 44-45-46-47-48)$$

$$NNO^+ + e^- \rightarrow NO^+(mass \quad 30-31-32) + N^+(mass \quad 14-15)$$

$$NNO^+ + e^- \rightarrow NN^+(mass \quad 28-29-30!!) + O^+(mass \quad 16-17-18)$$

Recombination's

Isotopic scrambling process

$$N^+ + O^+ \rightarrow NO^+(mass \quad 30-31-32)$$

$$NO^+ + O^+ \rightarrow NO_2^+(mass \quad 46-47)$$

The mass-to-charge peak signals which are present in the mass spectrum (fig.2) are the direct consequence of these process, and this was the starting point of defining our new approach for the complete characterization of N_2O and therefore to calculate the elemental isotopic abundances for Nitrogen and Oxygen.

The *scrambling* process is due to recombination between the ionic fragments in the source and as it is an effect which hampering the usual measurements for the mentioned masses, it will be discussed later in more detail.

The isotope amount ratios for the molecular mass-to-charge peaks - *m/z* = 44 to 48 are defined as:

$$
\begin{aligned}
{}^{45}R &= \frac{\left[x\left({}^{15}N\,{}^{14}N\,{}^{16}O\right)+x\left({}^{14}N\,{}^{15}N\,{}^{16}O\right)+x\left({}^{14}N_2\,{}^{17}O\right)\right]}{x\left({}^{14}N_2\,{}^{16}O\right)}\\
{}^{46}R &= \frac{\left[x\left({}^{15}N\,{}^{14}N\,{}^{17}O\right)+x\left({}^{14}N\,{}^{15}N\,{}^{17}O\right)+x\left({}^{14}N_2\,{}^{18}O\right)+x\left({}^{15}N_2\,{}^{16}O\right)\right]}{x\left({}^{14}N_2\,{}^{16}O\right)}\\
{}^{47}R &= \frac{\left[x\left({}^{15}N_2\,{}^{17}O\right)+x\left({}^{14}N\,{}^{15}N\,{}^{18}O\right)+x\left({}^{15}N\,{}^{14}N\,{}^{18}O\right)\right]}{x\left({}^{14}N_2\,{}^{16}O\right)}\\
{}^{48}R &= \frac{x\left({}^{15}N_2\,{}^{18}O\right)}{x\left({}^{14}N_2\,{}^{16}O\right)}
\end{aligned}
\qquad (1)
$$

where $x({}^{i}N^{j}N^{k}O)$ is defined as the fractional abundance of the individual N_2O species with

$$\sum_{i=14}^{15}\sum_{j=14}^{15}\sum_{k=16}^{18} x\left({}^{i}N\,{}^{j}N\,{}^{k}O\right)=1 \qquad (2)$$

Unfortunately, as it could be seen in fig.2, only three molecular mass-to-charge peaks could be detected and measured for usual Isotope Ratio Mass Spectrometer and therefore, only two Ratios could be determined.

However, the aim is to calculate the elemental isotope ratios which are defined as follows for Nitrogen and Oxygen:

$$
\begin{aligned}
{}^{15}R_1 &= \frac{\sum_{i=14}^{15}\sum_{k=16}^{18} x\left({}^{15}N\,{}^{i}N\,{}^{k}O\right)}{\sum_{i=14}^{15}\sum_{k=16}^{18} x\left({}^{14}N\,{}^{i}N\,{}^{k}O\right)}\\
{}^{15}R_2 &= \frac{\sum_{i=14}^{15}\sum_{k=16}^{18} x\left({}^{i}N\,{}^{15}N\,{}^{k}O\right)}{\sum_{i=14}^{15}\sum_{k=16}^{18} x\left({}^{i}N\,{}^{14}N\,{}^{k}O\right)}\\
{}^{17}R &= \frac{\sum_{i=14}^{15}\sum_{j=14}^{15} x\left({}^{i}N\,{}^{j}N\,{}^{17}O\right)}{\sum_{i=14}^{15}\sum_{j=14}^{15} x\left({}^{i}N\,{}^{j}N\,{}^{16}O\right)}\\
{}^{18}R &= \frac{\sum_{i=14}^{15}\sum_{j=14}^{15} x\left({}^{i}N\,{}^{j}N\,{}^{18}O\right)}{\sum_{i=14}^{15}\sum_{j=14}^{15} x\left({}^{i}N\,{}^{j}N\,{}^{16}O\right)}
\end{aligned}
\qquad (3)
$$

Taking into account the number of unknowns - the fractional abundances for Nitrogen – ${}^{15}R_1$ and ${}^{15}R_2$ –for the central and terminal position, and Oxygen – ${}^{17}R$ and ${}^{18}R$, it would results, at a first sight, that four equations are needed to be solved and therefore at least four isotope ratios have to be measured, in order to complete the isotope characterization of Nitrous oxide.

It must be noted that, using common Isotope Ratio Mass Spectrometer, with a resolution ($m/\Delta m$ of about 200, it is impossible to distinguish between species with the same molecular mass number. Therefore, the elemental isotope ratios cannot be derived simply from only measurements of ^{45}R and ^{46}R, without additional assumptions.

Instead, the proposed approach for this project only contains basic general accepted assumption – a complete statistical isotope distribution between different isotopologues.

Assuming such a statistical distribution, the relative abundance of individual N_2O species can be factorized and calculated as follows:

$$\begin{aligned} {}^{45}R &= {}^{15}R_1 + {}^{15}R_2 + {}^{17}R \\ {}^{46}R &= \left({}^{15}R_1 + {}^{15}R_2\right)\cdot{}^{17}R + {}^{18}R + {}^{15}R_1 \cdot {}^{15}R_2 \\ {}^{47}R &= \left({}^{15}R_1 + {}^{15}R_2\right)\cdot{}^{18}R + {}^{15}R_1 \cdot {}^{15}R_2 \cdot {}^{17}R \\ {}^{48}R &= {}^{15}R_1 \cdot {}^{15}R_2 \cdot {}^{18}R \end{aligned} \qquad (4)$$

Obviously, even if we assume complete isotope statistical distribution, the equation system is still underestimated. Therefore, taking into account the new analytical capabilities of MAT 271-IRMS, the fragment analysis will be the right option to avoid the problems related to supplementary assumptions.

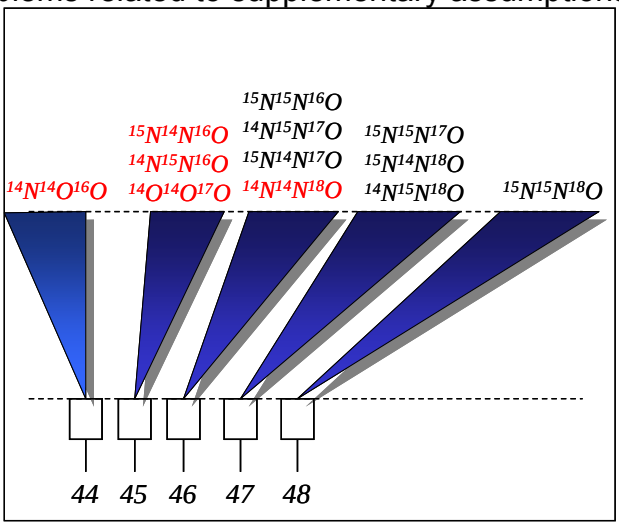

Figure 3.: Schematic presentation of the N_2O isotopomers distribution on the mass-to-charge signals

Fragment analysis (if the instrumental sensitivity allows) could provide additional equations to complete the equation system for elemental isotope abundances. From the N_2O mass spectrum it could be noticed that next to the N_2O^+ molecular ions, the following significant fragments are produced due to the process mentioned in the electron impact ion source – NO^+ (~32%), N_2^+ (~7%), N^+(~11%) and O^+(~3%). The most important ion fragment for our analytical purpose was considered NO^+ - mass-to-charge 30, 31 and 32, as the intramolecular ^{15}N distribution could be determined from this ion fragment. Also, the N_2^+ fragment (*m/z* 28 and 29) was used within the measurement method as additional isotope ratios which could bring new equations for the final mathematical treatment. In the case of NO^+, as it was mentioned, some isotopic scrambling requires a correction for which must be performed by using an additional s –"*scrambling coefficient*". Using this new parameter, the data treatment for the NO^+ fragment isotope ratio measurements – ^{31}R and ^{32}R was reformulated, as follows:

$$
{}^{31}R = \frac{s\cdot\left(x\left({}^{15}NN^{16}O\right)+x\left({}^{14}NN^{17}O\right)\right)+(1-s)\cdot\left(x\left(N^{15}N^{16}O\right)+x\left(N^{14}N^{17}O\right)\right)}{s\cdot x\left({}^{14}NN^{16}O\right)+(1-s)\cdot x\left(N^{14}N^{16}O\right)} =
$$

$$
={}^{17}R+\frac{s\cdot x\left({}^{15}NN^{16}O\right)+(1-s)\cdot x\left(N^{15}N^{16}O\right)}{s\cdot x\left({}^{14}NN^{16}O\right)+(1-s)\cdot x\left(N^{14}N^{16}O\right)}={}^{17}R+\frac{s\cdot\frac{{}^{15}N^{14}N^{16}O+{}^{15}N^{15}N^{16}O}{{}^{14}N^{14}N^{16}O}+(1-s)\cdot\frac{{}^{15}N^{15}N^{16}O+{}^{14}N^{15}N^{16}O}{{}^{14}N^{14}N^{16}O}}{s\cdot\frac{{}^{14}N^{14}N^{16}O+{}^{14}N^{15}N^{16}O}{{}^{14}N^{14}N^{16}O}+(1-s)\cdot\frac{{}^{14}N^{14}N^{16}O+{}^{15}N^{14}N^{16}O}{{}^{14}N^{14}N^{16}O}} =
$$

$$
={}^{17}R+\frac{s\cdot\left({}^{15}R_1+{}^{15}R_1\cdot{}^{15}R_2\right)+(1-s)\cdot\left({}^{15}R_1\cdot{}^{15}R_2+{}^{15}R_2\right)}{s\cdot\left(1+{}^{15}R_2\right)+(1-s)\cdot\left(1+{}^{15}R_1\right)} =
$$

$$
={}^{17}R+\frac{s\cdot{}^{15}R_1+(1-s)\cdot{}^{15}R_2+{}^{15}R_1\cdot{}^{15}R_2}{1+s\cdot{}^{15}R_2+(1-s)\cdot{}^{15}R_1} =
$$

$$
={}^{17}R+\frac{s\cdot{}^{15}R_1+s^2\cdot{}^{15}R_1\cdot{}^{15}R_2-s^2\cdot{}^{15}R_1\cdot{}^{15}R_2+s\cdot(1-s)\cdot{}^{15}R_1^2-s\cdot(1-s)\cdot{}^{15}R_1^2+(1-s)\cdot{}^{15}R_2+{}^{15}R_1\cdot{}^{15}R_2}{1+s\cdot{}^{15}R_2+(1-s)\cdot{}^{15}R_1} =
$$

$$
={}^{17}R+s\cdot{}^{15}R_1+\frac{(1-s)\cdot{}^{15}R_2+{}^{15}R_1\cdot{}^{15}R_2\cdot\left(1-s^2\right)-s\cdot(1-s)\cdot{}^{15}R_1^2}{1+s\cdot{}^{15}R_2+(1-s)\cdot{}^{15}R_1} =
$$

$$
={}^{17}R+s\cdot{}^{15}R_1+\frac{(1-s)\cdot{}^{15}R_2+s\cdot(1-s)\cdot{}^{15}R_2^2-s\cdot(1-s)\cdot{}^{15}R_2^2+(1-s)^2\cdot{}^{15}R_1\cdot{}^{15}R_2-(1-s)^2\cdot{}^{15}R_1\cdot{}^{15}R_2+\left(1-s^2\right)\cdot{}^{15}R_1\cdot{}^{15}R_2-s\cdot(1-s)\cdot{}^{15}R_1^2}{1+s\cdot{}^{15}R_2+(1-s)\cdot{}^{15}R_1} =
$$

$$
={}^{17}R+s\cdot{}^{15}R_1+(1-s)\cdot{}^{15}R_2+\frac{{}^{15}R_1\cdot{}^{15}R_2\cdot\left[\left(1-s^2\right)-(1-s)^2\right]-s\cdot(1-s)\cdot{}^{15}R_1^2-s\cdot(1-s)\cdot{}^{15}R_2^2}{1+s\cdot{}^{15}R_2+(1-s)\cdot{}^{15}R_1} =
$$

$$
={}^{17}R+s\cdot{}^{15}R_1+(1-s)\cdot{}^{15}R_2-\frac{s\cdot(1-s)\cdot\left[{}^{15}R_1-{}^{15}R_2\right]^2}{1+s\cdot{}^{15}R_2+(1-s)\cdot{}^{15}R_1}
$$

(5)

and

$$
{}^{32}R = \frac{s\cdot\left(x\left({}^{15}NN^{17}O\right)+x\left({}^{14}NN^{18}O\right)\right)+(1-s)\cdot\left(x\left(N^{15}N^{17}O\right)+x\left(N^{14}N^{18}O\right)\right)}{s\cdot x\left({}^{14}NN^{16}O\right)+(1-s)\cdot x\left(N^{14}N^{16}O\right)} =
$$

$$
{}^{18}R+\frac{s\cdot x\left({}^{15}NN^{17}O\right)+(1-s)\cdot x\left(N^{15}N^{17}O\right)}{s\cdot x\left({}^{14}NN^{16}O\right)+(1-s)\cdot x\left(N^{14}N^{16}O\right)} =
$$

$$
={}^{18}R+\frac{s\cdot\frac{{}^{15}N^{14}N^{17}O+{}^{15}N^{15}N^{17}O}{{}^{14}N^{14}N^{16}O}+(1-s)\cdot\frac{{}^{14}N^{15}N^{17}O+{}^{15}N^{15}N^{17}O}{{}^{14}N^{14}N^{16}O}}{s\cdot\frac{{}^{14}N^{14}N^{16}O+{}^{14}N^{15}N^{16}O}{{}^{14}N^{14}N^{16}O}+(1-s)\cdot\frac{{}^{14}N^{14}N^{16}O+{}^{15}N^{14}N^{16}O}{{}^{14}N^{14}N^{16}O}} =
$$

$$
{}^{18}R+\frac{s\cdot\left({}^{15}R_1\cdot{}^{17}R+{}^{15}R_1\cdot{}^{15}R_2\cdot{}^{17}R\right)+(1-s)\cdot\left({}^{15}R_2\cdot{}^{17}R+{}^{15}R_1\cdot{}^{15}R_2\cdot{}^{17}R\right)}{s\cdot\left(1+{}^{15}R_2\right)+(1-s)\cdot\left(1+{}^{15}R_1\right)} =
$$

$$
={}^{18}R+\frac{{}^{15}R_1\cdot{}^{15}R_2\cdot{}^{17}R+s\cdot{}^{15}R_1\cdot{}^{17}R+(1-s)\cdot{}^{15}R_2\cdot{}^{17}R}{1+s\cdot{}^{15}R_2+(1-s)\cdot{}^{15}R_1} =
$$

$$
{}^{18}R+{}^{17}R\cdot\left[\frac{{}^{15}R_1\cdot{}^{15}R_2+s\cdot{}^{15}R_1+(1-s)\cdot{}^{15}R_2}{1+s\cdot{}^{15}R_2+(1-s)\cdot{}^{15}R_1}\right]={}^{18}R+{}^{17}R\cdot\left[s\cdot{}^{15}R_1+(1-s)\cdot{}^{15}R_2-\frac{s\cdot(1-s)\cdot\left[{}^{15}R_1-{}^{15}R_2\right]^2}{1+s\cdot{}^{15}R_2+(1-s)\cdot{}^{15}R_1}\right]
$$

(6)

where

$$
{}^{31}R=\frac{I^{31}}{I^{30}}
$$

$$
{}^{32}R=\frac{I^{32}}{I^{30}}
$$

(7)

are the measured NO^+ isotopic ion fragment ratios.

In a similar way, N_2^+ fragments (*m/z* 28 and 29) are used to obtain an additional equation:

$$^{29}R = \frac{I^{29}}{I^{28}} = \frac{x\left(^{15}N^{14}N\right)}{x\left(^{14}N^{14}N\right)} = {}^{15}R_1 + {}^{15}R_2 \quad (8)$$

Therefore, to summarize, a set of distinct isotope ratio measurements for N_2O gas has been elaborated and performed in order to define a determinate equation systems to be solved for the Nitrogen and Oxygen elemental isotopic abundances.

However, a series of analytical issues had to be solved for an accurate measurement of the mentioned mass-to-charge peak signals;

1.1 CO_2 contribution at mass-to-charge 44, 45 and 46.

For normal atmospheric N_2O samples, even after extraction and purification, the N_2O sample will contain significant high contents of CO_2. This is due to the similarity between the vapor pressure curves of both gases which makes them impossible to separate by cryogenic techniques and of the much higher concentration of CO_2 in air (~ 1000 times higher than of Nitrous oxide). Therefore, the CO_2 "*contamination*" in atmospheric N_2O samples is highly probable and special care has to be taken to correct for it.

The most adequate method to eliminate the contribution of CO_2 isotopomers was to investigate the molecular mass-to-charge peak signals 44, 45 and 46 in an experiment sequence with an additional mass-to-charge peak signal measurement at *m/z=12*. This mass-to-charge is the single one present in the mass spectrum of CO_2 but not in the mass spectrum of N_2O. Therefore, using this opportunity, a distinct isotope ratio measurement has been done on a pure CO_2 gas sample in order to calculate the time dependence of isotope ratios 44/12, 45/12 and 46/12 respectively. These isotope ratios time sequence have been used as correction factors for the main isotope ratio measurement, according to the following relations:

$$R_{45/44}(i) = \frac{I_{45}(i) - I_{45-backg} - I_{12}(i) \cdot f_{F/S} \cdot F_{45/12}}{I_{44}(i) - I_{44-backg} - I_{12}(i) \cdot f_{F/S} \cdot F_{44/12}}$$

$$R_{46/44}(i) = \frac{I_{46}(i) - I_{46-backg} - I_{12}(i) \cdot f_{F/S} \cdot F_{46/12}}{I_{44}(i) - I_{44-backg} - I_{12}(i) \cdot f_{F/S} \cdot F_{44/12}} \quad (9)$$

where

- $I_{44\text{-backg}}$, $I_{45\text{-backg}}$ and $I_{46\text{-backg}}$ are the corrections for the instrumental background
- $F_{F/S}$ – calibration factor between the two detectors used during measurements – Faraday and Secondary Electron Multiplier in Ion Counting mode, and
- $F_{44/12}$, $F_{45/12}$ and $F_{46/12}$ are the isotope ratios time dependence for the pure CO_2 gas sample measurement

In fig.4 and 5 an uncorrected and corrected for CO_2 44 mass-to-charge intensity is shown function of time. Even at the first sight, no difference could be noticed; the corrected values are 0.01% lower than the uncorrected ones.

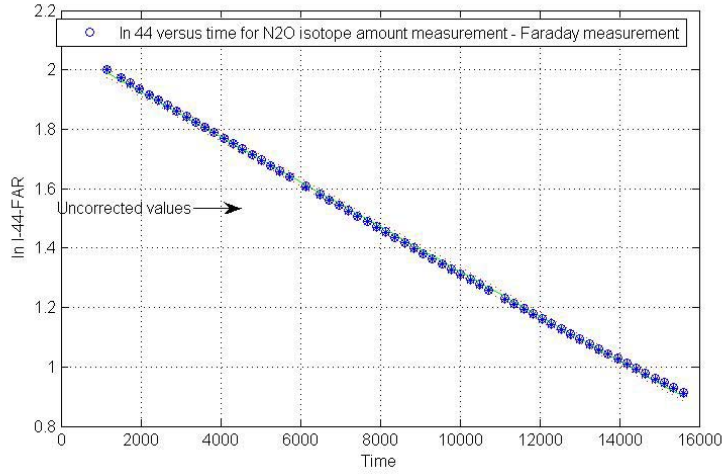

Fig.4.: Mass-to-charge intensity 44 versus time for a N_2O isotope ratio measurement – presented on a logarithmic scale

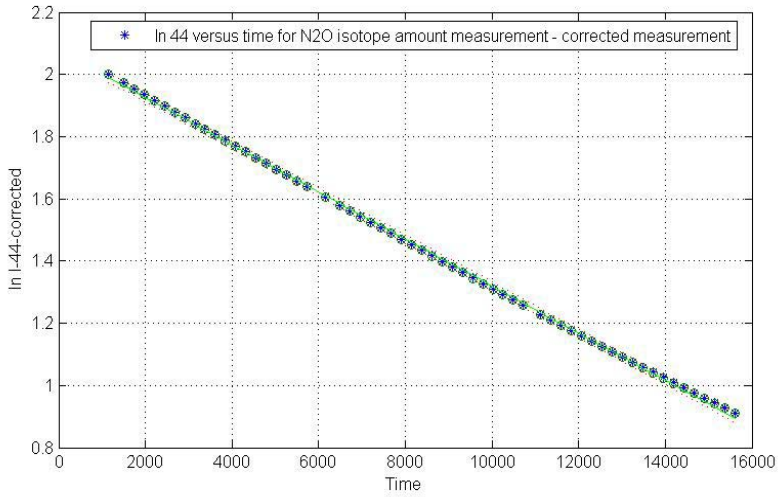

Figure 5.: Mass-to-charge 44 intensity versus time, for N_2O isotope ratio measurement – signal corrected for CO_2 presence in the gas sample, using the relationship (9)

1.2 Ion-molecule reaction product

As mentioned before, the fragmentation and recombination processes, which occur in the electron impact ion source, represent a disturbing factor for isotope ratio measurements. Between these processes, the production of NO_2^+ as a result of ion-molecule reactions will obstruct especially the measurements of 46 mass-to-charge intensity:

$$N_2O + O^+ \rightarrow NO_2^+ + N^+$$
$$N_2O + NO^+ \rightarrow NO_2^+ + N_2^+ \quad (10)$$

In order to adjust the measured 46 mass-to-charge intensity by extracting the contribution of this ion-molecule reaction product, a mathematical data treatment was elaborated starting from the measurement basic principle of MAT271 IRMS. The unique character of this IRMS is given by its capability of measuring a given mass-to-charge peak signals sequence, successively in time, and relating the data row to the molecular gas flow principle. According to Knudsen molecular gas flow theory, the amount of gas in the inlet system vessel will decrease exponentially, with an exponent factor proportional to the square root of the molecular mass.

Therefore, if a certain signal is a result of a ion-molecule reaction in the electron impact ion source, the decrease of its intensity will be with an exponential factor depending of the product of the molecular masses of the participant of this reaction. For the particular case of interest (reaction 10), it will result:

$$\frac{I_{NO^+}}{\left(I_{NO^+}\right)_0} = e^{-k_{44}\cdot t}$$

$$\frac{I_{O^+}}{\left(I_{O^+}\right)_0} = e^{-k_{44}\cdot t} \qquad (11)$$

as the ion fragments NO^+ and O^+ are both resulted from the $^{14}N_2{}^{16}O$ (molecular mass 44) gas. Therefore, the signal given by the ions resulted in the ion-molecule reaction (recombination in the electron impact ion source) will have a time evolution according to the following relationship:

$$\frac{I_{NO_2^+}}{\left(I_{NO_2^+}\right)_0} = \left(e^{-k_{44}\cdot t}\right)^2 = e^{-2\cdot k_{44}\cdot t} \qquad (12)$$

or

$$\ln\left(I_{NO_2^+}\right) - \ln\left(I^0_{NO_2^+}\right) = -2\cdot k_{44}\cdot t$$

The 46 mass-to-charge peak signal measured on MAT 271 will be therefore a sum of the contribution given by the N_2O^+ ions of mass–to-charge 46, itself and a small additional part produced by the ion-molecule reactions described.

The main contribution from the isotopomers of Nitrous oxide of mass-to-charge 46 will have an exponential time decrease according to the relation:

$$\ln\left(I^{46}_{N_2O^+}\right) - \ln\left(I^{46}_{N_2O}\right)_o = -k_{46}\cdot t \qquad (13)$$

The 46 mass-to-charge signal time sequence measured on MAT 271 IRMS will obey therefore the bellow relationship:

$$I_{46} = I^{46}_{N_2O^+} + I^{46}_{NO_2^+} = \left(I^{46}_{N_2O^+}\right)_0 \cdot e^{-k_{46}t} + \left(I^{46}_{NO_2^+}\right)_0 \cdot e^{-2k_{44}t} \qquad (14)$$

A required correction for the ion-molecule product to the 46 signal needs a precisely estimation of the second part of relation 14 and an extraction afterwards. The challenge of this part of the work was to calculate the leak rate k_{46} using only the raw data –intensities and time values (a set of I_{46} and t).

A logarithmic plot of the signal time sequence measured, versus time will reveal the leak rate constant for the investigated mass-to-charge peak. For example, the slope of the linear regression of logarithmic plot of mass-to-charge 44 peak signal will be used to calculate the 44 mass-to-charge leak rate – k_{44}.

A numerical derivation of the 46 mass-to-charge peak intensity, will transform relation 14 into:

$$\frac{dI_{46}}{dt} = \frac{\Delta I_{46}}{\Delta t} = -\left(I^{46}_{N_2O^+}\right)_0 \cdot k_{46} \cdot e^{-k_{46}\cdot t} - 2\cdot\left(I^{46}_{NO_2^+}\right)_0 \cdot k_{44} \cdot e^{-2\cdot k_{44}\cdot t} \qquad (15)$$

Multiplying eq. 14 by k_{44} and summing term by term the last two relations, will result:

$$\ln\left[\frac{\Delta I_{46}}{\Delta t} + 2\cdot k_{44}\cdot I_{46}\right] = -k_{46}\cdot t + \ln\left[\left(I^{46}_{N_2O^+}\right)_0 \cdot \left(2\cdot k_{44} - k_{46}\right)\right] \qquad (16)$$

which is the theoretical basis for calculation of leak rate k_{46}. Therefore, within the data treatment software which has been elaborated for this purpose, such procedure has been inserted to numerical derivate the time sequence of intensity

46 and finally a linear regression of $\ln\left[\frac{\Delta I_{46}}{\Delta t} + 2 \cdot k_{44} \cdot I_{46}\right]$ versus time, will reveal the required k_{46}. It must be noticed that k_{44} from the above relation has been calculated previously from the slope of the logarithmic plot of I_{44} function of time.

In fig.6, the described linear regression, applied for one of the N_2O isotope ratio measurements could be seen. It must be noticed that the experimental data were in good agreement with the theoretical model applied for this particular correction.

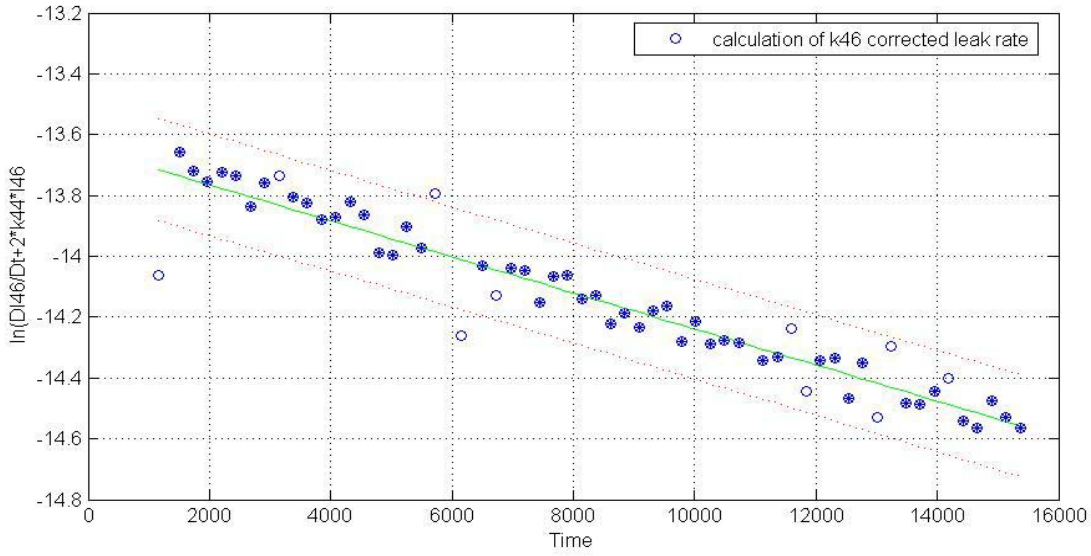

Figure 6.: Linear regression those slope is the required k_{46}

Once the real leak rate for mass-to-charge 46 has been determined, corrected for ion-molecule products, the same set of equations (14-15) has been used to evaluate the intensities at t=0 - $\left(I^{46}_{N_2O}\right)_0$. By a simple mathematical treatment of the two equations 14-15 it will result in:

$$\frac{I_{46}}{e^{-2\cdot k_{44}\cdot t}} = \left(I^{46}_{N_2O^+}\right)_0 \cdot e^{-(k_{46}-2\cdot k_{44})\cdot t} + \left(I^{46}_{NO_2^+}\right)_0 \qquad (17)$$

and therefore a linear regression of the plot of the left term in the equation above, the function $e^{-(k_{46}-2\cdot k_{44})t}$ was used for the calculation of $\left(I^{46}_{N_2O^+}\right)_0$. Finally, the 46 mass-to-charge signal corrected for ion-molecule product NO_2^+ is given by:

$$I^{correct}_{46}(i) = I_{46}(i) - \left(I^{46}_{NO_2^+}\right)_0 \cdot e^{-2\cdot k_{44}\cdot t(i)} \qquad (18)$$

It must be emphases that the entire described mathematical treatment for NO_2^+ correction for the signal measured at 46 mass-to-charges has been included numerically in the general software for N_2O measurement and has been elaborated to be applied in the same time sequence as the other peak signals acquired. In figure 7 and 8, two distinct plot of mass-to-charge 46 are shown-the first one without any ion-molecule reaction correction and the other after applying it.

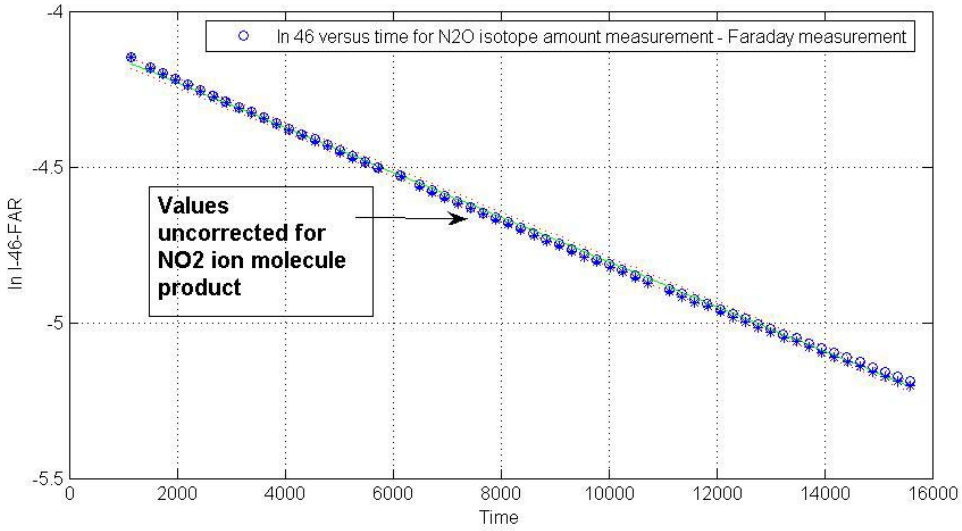

Figure 7: Time sequence for the 46 mass-to-charge signal acquired on MAT 271 for the Nitrous oxide isotope ratio measurement - uncorrected values. The "bending" of the logarithmic plot is due to the deviation produced by ion-molecule reactions which has contribution to this mass-to-charge

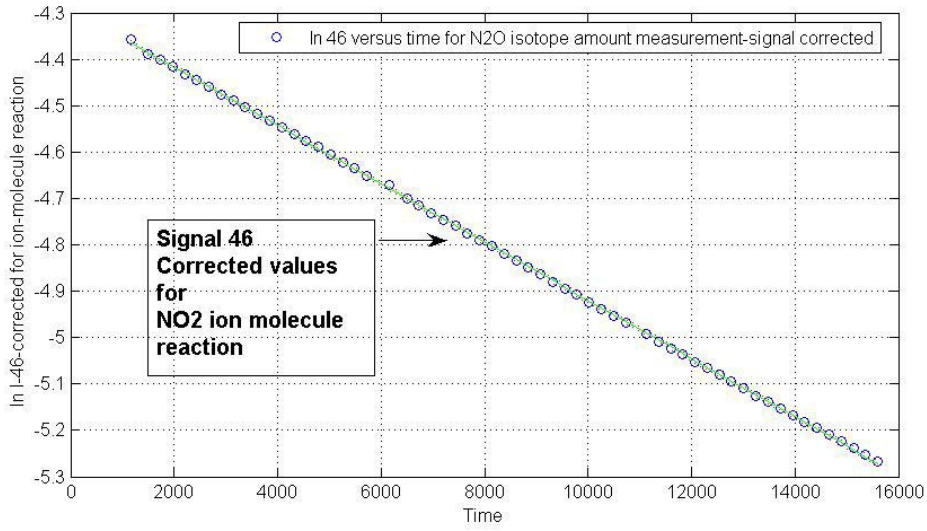

Figure 8: The same 46 mass-to-charge signal, corrected for NO_2^+ produced in the ion-molecule reaction in the electron impact ion source. The time evolution of the signal is very "close" to the linear theoretical prediction

1.3 Treatment of "Isotope scrambling effect"

The fragmentation followed by recombination processes in the electron impact ion source is a disturbing effect which generally influence strongly the position-dependent isotope ratio measurements. An illustrative case for the "scrambling" process is Nitrous oxide, where the isotope ratio measurement for NO^+ fragment ions requires a special treatment and correction for the mixing process between the Nitrogen atoms – terminal and central one, bound to Oxygen atom. As it was mentioned, due to the extremely small signals for mass-to-charge 47 and 48, a distinct ion fragment isotope ratio measurement had to be applied to complete the equation system for solving for the four elemental fractional abundances – $^{15}N_1$, $^{15}N_2$, ^{17}O and ^{18}O. Unfortunately, the welcome fact that the main ion fragments NO^+ contain mainly the central Nitrogen atoms and therefore an isotope ratio measurement for mass-to-charge 30 and 31 will provide the required equation for $^{15}N_2$ determination, is hampered by the "scrambling" effect:

$$^{i}N-^{j}N-^{k}O \xrightarrow{fragmentation} {}^{j}N-^{k}O+{}^{i}N \xrightarrow{further\ \ fragmentation} {}^{j}N+^{k}O$$

$$^{j}N+^{k}O \xrightarrow{recombination} {}^{j}N-^{k}O$$

From the potential example described above, it could be seen that the statistical distribution of the central Nitrogen atom within NO^+ fragment is disturbed by the probability of recombination process that involve a terminal Nitrogen atom.

In order to adequately treat this process and take into account the "scrambling" isotopic effect, a new coefficient has been introduced in the calculation as an additional unknown. This "scrambling" factor was defined as the probability that N^+ and O^+ could recombine and contribute therefore at mass-to-charge position 30, additional to the NO^+ ions coming from the bonding break N-NO – dissociative ionization. Using this coefficient, and according to eq.5 and 6, the isotope ratio for ion fragment NO^+ is written as follows:

$$^{31}R=^{17}R+s\cdot{}^{15}R_1+(1-s)\cdot{}^{15}R_2-\frac{s\cdot(1-s)\cdot\left[{}^{15}R_1-{}^{15}R_2\right]^2}{1+s\cdot{}^{15}R_2+(1-s)\cdot{}^{15}R_1} \tag{19}$$

$$^{32}R=^{18}R+{}^{17}R\cdot\left[s\cdot{}^{15}R_1+(1-s)\cdot{}^{15}R_2-\frac{s\cdot(1-s)\cdot\left[{}^{15}R_1-{}^{15}R_2\right]^2}{1+s\cdot{}^{15}R_2+(1-s)\cdot{}^{15}R_1}\right] \tag{20}$$

These two equations were added to those which express the elemental fractional abundances using the acquired isotope ratios R_{45} and R_{46}.

1.4 Correction for the Nitrogen impurity in the Nitrous oxide sample

As the number of equations to be solve for elemental fractional abundances is not sufficient due to the additional unknown – "scrambling coefficient", a supplementary measurement experiment has been elaborated and included in the overall procedure This new isotope ratio measurement involves the acquisition of 28 and 29 mass-to-charge signals, which are produced by the N_2^+ ion fragments. Expressing the isotope ratio $^{29}R=\frac{I^{29}_{N_2}}{I^{28}_{N_2}}$ using the fractional abundances will result the following simple relation:

$$^{29}R=^{15}R_1+{}^{15}R_2 \tag{21}$$

However, the simplicity of this equation was counterbalanced by the difficulty to correctly measuring the signals for 28 and 29 mass-to-charges, which is coming only from the N_2^+ ion fragment originate from Nitrous oxide sample. It is well-known that the main component of the usual IRMS background is Nitrogen 28 signal and therefore, this must be extracted from the real measurement. Moreover, the probable (the usual samples are atmospheric ones and Nitrogen is the main component of it) Nitrogen impurity in the Nitrous oxide sample is expected to come with an additional contribution to the 28 and 29 mass-to-charge signals. A distinct measurement for MAT 271 background for the peak signals of interest has been done periodically, and the time-corrected values have been automatically extracted (by the data treatment software).

In order to correct for the potential Nitrogen impurity originating from the Nitrous oxide sample, we developed and used a procedure similar to that applied to correct for ion-molecule reaction product. To exemplify it, we will only show the basics of this method for mass-to-charge signal 28. The acquired signal is supposed to be given by the contributions of two terms:

$$I^{28}=I^{28}_{N_2^+}(N_2)+I^{28}_{N_2^+}(N_2O) \tag{22}$$

At the first sight it is impossible to distinguish between the signals given by two ions with absolutely the same molecular mass, but the peculiar feature of MAT 271 IRMS allowed us to elaborate the right method for correcting the 28 and 29 mass-to-charge signals. According to Knudsen molecular gas flow law, the time evolution of I^{28} is described by the following relationship:

$$I^{28} = \left[I^{28}_{N_2^+}\left(N_2\right)\right]_o \cdot e^{-k_{28}\cdot t} + \left[I^{28}_{N_2^+}\left(N_2O\right)\right]_o \cdot e^{-k_{44}\cdot t} \tag{23}$$

A numerical time differentiation of the acquired 28 mass-to-charge signal will transform (23) into:

$$\frac{dI^{28}}{dt} = \frac{\Delta I^{28}}{\Delta t} = \frac{I^{28}_{n+1} - I^{28}_{n}}{t_{n+1} - t_n} = -k_{28} \cdot \left[I^{28}_{N_2^+}\left(N_2\right)\right]_o \cdot e^{-k_{28}\cdot t} - k_{44} \cdot \left[I^{28}_{N_2^+}\left(N_2O\right)\right]_o \cdot e^{-k_{44}\cdot t} \tag{24}$$

where I_n and t_n are the n-th signal and time value acquired in the sequence, on MAT 271. Multiplying (23) by k_{44} and summing the last two equations will result:

$$k_{44} \cdot I^{28} + \frac{dI^{28}}{dt} = \left(k_{44} - k_{28}\right) \cdot \left[I^{28}_{N_2^+}\left(N_2\right)\right]_o \cdot e^{-k_{28}\cdot t} \tag{25}$$

or, applying logarithm to both terms will result

$$\ln\left(k_{44} \cdot I^{28} + \frac{dI^{28}}{dt}\right) = -k_{28} \cdot t + \ln\left[\left(k_{44} - k_{28}\right) \cdot \left(I^{28}_{N_2^+}\right)_o\right] \tag{26}$$

Keeping in mind that k_{44} has been calculated already from the 44 mass-to-charge signal time evolution, all the values from the left term in eq.(26) are known. Therefore, a linear regression of the plot of this term function of time will be used to calculate the k_{28} leak rate. In a similar way, using the two equations (23) and (24), will reveal the computation of $\left[I^{28}_{N_2^+}\left(N_2\right)\right]_o$. Once these two parameters are calculated, the correction for Nitrogen impurities in the Nitrous oxide sample is straightforwardly applied by:

$$\left(I^{28}\right)_{corrected} = \left(I^{28}\right)_{measured} - \left[I^{28}_{N_2^+}\left(N_2\right)\right]_o \cdot e^{-k_{28}\cdot t} \tag{27}$$

To summarize, the Nitrous oxide isotopic characterization procedure developed and applied within this research project is based on several measurement experiments for molecular mass ions (mass-to-charge 44, 45 and 46) and fragment ions (mass-to-charge 28 and 289 for N_2^+ fragments and 30, 31 and 32 for NO^+ fragments respectively). Required corrections has been taken into account for potential impurities in the samples – CO_2 with a direct effect onto masses 44 45 and 46 and N_2 for fragment isotope ratio measurement 28 and 29.

Also, background correction has been applied in the time sequence for all the signals of interest. A special procedure has been developed for eliminate the effect of disturbance produced by ion-molecule reaction in the electron impact ion source, those products NO_2^+ have a significant contribution to 46 mass-to-charge signal. The final equation system that was used to uniquely solve for elemental fractional abundances of Nitrogen and Oxygen in Nitrous oxide is as follows:

$$\begin{aligned}
{}^{45}R &= {}^{15}R_1 + {}^{15}R_2 + {}^{17}R \\
{}^{46}R &= \left({}^{15}R_1 + {}^{15}R_2\right) \cdot {}^{17}R + {}^{18}R + {}^{15}R_1 \cdot {}^{15}R_2 \\
{}^{31}R &= {}^{17}R + s \cdot {}^{15}R_1 + \left(1-s\right) \cdot {}^{15}R_2 - \frac{s \cdot \left(1-s\right) \cdot \left[{}^{15}R_1 - {}^{15}R_2\right]^2}{1 + s \cdot {}^{15}R_2 + \left(1-s\right) \cdot {}^{15}R_1}
\end{aligned}$$

$$^{32}R = {}^{18}R + {}^{17}R \cdot \left[s \cdot {}^{15}R_1 + (1-s) \cdot {}^{15}R_2 - \frac{s \cdot (1-s) \cdot \left[{}^{15}R_1 - {}^{15}R_2 \right]^2}{1 + s \cdot {}^{15}R_2 + (1-s) \cdot {}^{15}R_1} \right]$$

$$^{29}R = {}^{15}R_1 + {}^{15}R_2 \qquad (28)$$

All the corrections before mentioned with the mathematical treatment has been included in a unique software which automatically use as input data the file resulted from the raw data acquisition on MAT 271 on every experiment elaborated and provide the finals values for elemental fractional abundances $^{15}R_1$, $^{15}R_2$, ^{17}R and ^{18}R. Even the data are resulted from distinct measurements for the same sample, the data treatment is correcting it for time drifting, all the elements of the data vectors being averaged and evaluated at the same time values.

2. MAT 271 – IRMS analytical improvements

Directly related to the main goal of the research project, several hardware and software improvements have been implemented for MAT 271 IRMS. The objective of these improvements was to extend the range of isotope ratios measurements in order to allow the measurement of 46/44 for N_2O samples and on the other hand to measure very low mass-to-charge signals as required for a precisely background correction. Obviously, the main improvement has been done for the detection system. The original status of MAT 271 detection system was with a single detection line based on Faraday cup, with an amplification factor of 10^{10}. (fig.9)

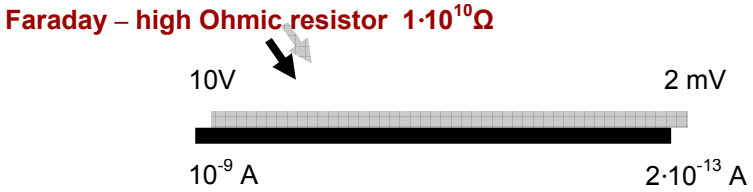

Figure 9.: The isotope amount ratio range for MAT 271 –original status

Such configuration was used to measure isotope amount ratio until $2\text{-}5*10^{-4}$ which is totally not sufficient for the present analytical purposes. Therefore, a first improvement which has been implemented for MAT 271 during 2005 was to introduce an additional Secondary Electron Multiplier in a Ion counting mode detection system. The new system needed new acquisition software in order to allow a mass-to-charge peak signals sequence for different detection system and also, by introducing a dynamic Faraday-SEM calibration.

The dynamic calibration involved to measure during the peak sequence acquisition a same mass-to-charge peak signal on both detectors and a dynamic ratio between these signals will be applied for conversion between counts and voltage values. In this way, the system is able to measure isotope amount ratio until 10^{-6} (until ppm level) and practically a large field of isotope ratio measurement was opened in this way – precise background measurements, isotope ratios which involves very rare isotopomers in natural samples and highly enriched sample (fig.10)

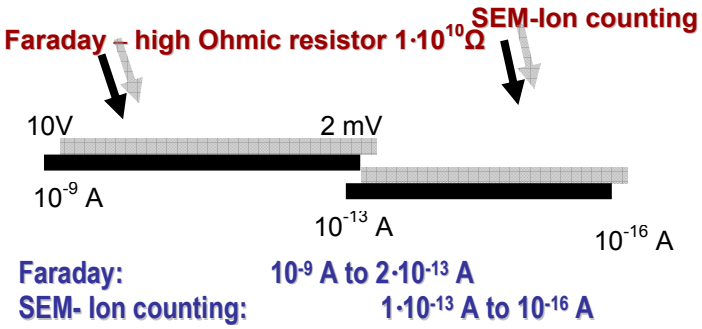

Figure 10: Two detection system implemented for MAT271 and extending the isotope amount ratio until 10^{-6}

However, for low intensity signals, the poor statistics of the number of counts acquired on SEM-Ion counter produced large uncertainties for the resulted isotope amount ratios. Also, the small extend of the overlapping range between the two detection systems (see fig.10) made it extremely difficult to achieve a good dynamical calibration factor. The opportunity to have within the measured mass spectrum, a peak signal that has the right intensity to be accurately acquired on both detectors is not often achieved. Therefore, a second step for hardware improvement for MAT 271 has been projected and applied. The basic idea was to insert a new detection channel on the same Faraday cup detector, but with an intermediate amplification factor (see fig.11). In this way, according to the peak signals intensities, the new measurement experiment divide it on three detection system with larger overlapping intervals and dynamical calibration factors are calculated between the two Faraday channels(high and low amplification) and between the Faraday and SEM-Ion counter detectors. A dynamical measurement range of 10^7 has been achieved in this way.

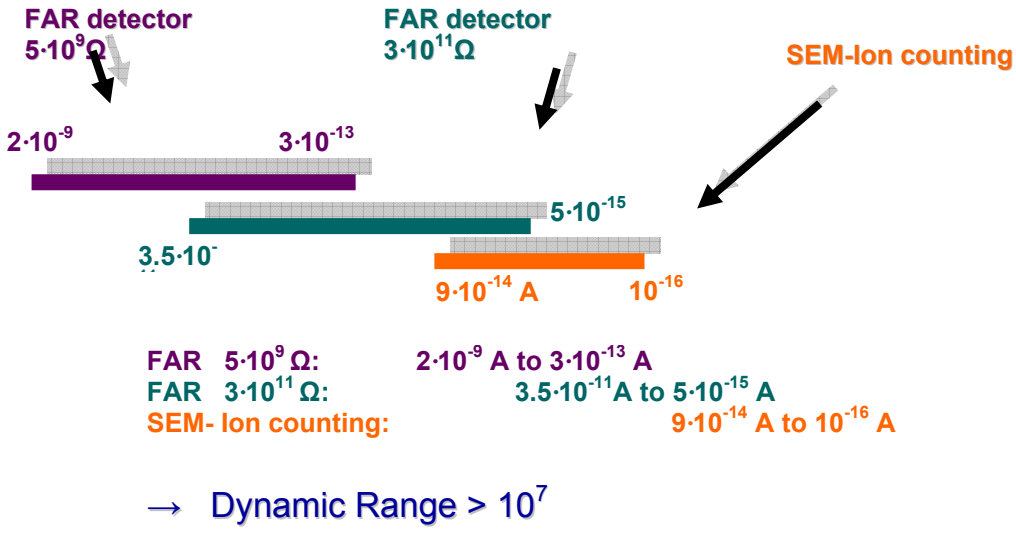

Figure 11. : The new detection configuration on MAT 271 IRMS with two detection channels (for the same Faraday cup) and a SEM-Ion counter system for very low intensity signals

The main advantage of this new detection setup was the possibility for a better dynamical calibration between the detectors. The overlapping interval that allows the dynamical calibration is significantly extended (fig.12) and by choosing an adequate inlet pressure, the right intensity signals for the “link” peaks could be

achieved. Moreover, we have the option to avoid the use of SEM-Ion counter (which by its feature always introduce larger measurement uncertainty) and involve only the two Faraday detection channels.

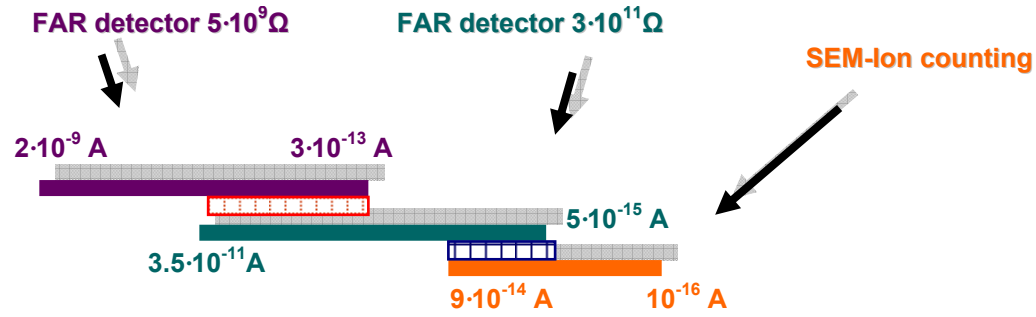

Figure 12.: The overlapping interval for the detection configuration on MAT 271, used for setting adequate "link" peak within the measurement experiment for an accurate dynamical calibration

The practical idea which allows the inserting of a new detection channel on the same Faraday cup, with a different amplification factor, was to use a computer controlled switch (fig.13) which made the option available for choosing between a single high amplification resistor or a combination of two such amplification resistors in parallel. Therefore, during the experiment development, the computer will command the switch and use the right detection channel for the measured mass-to-charge peak signal.

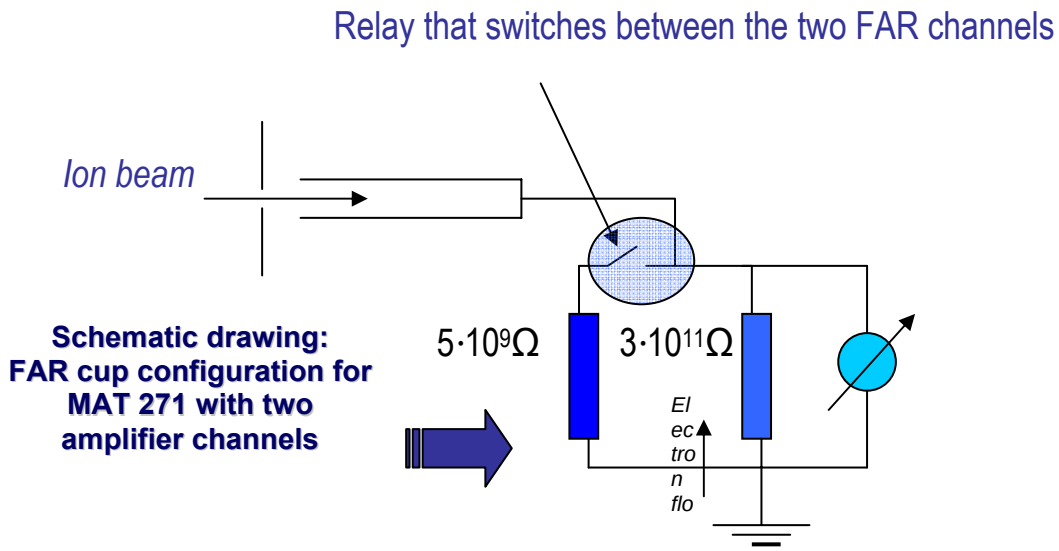

Figure 13.: Schematic view of the experimental setup used for implementing two detection channels on the same Faraday cup for MAT 271

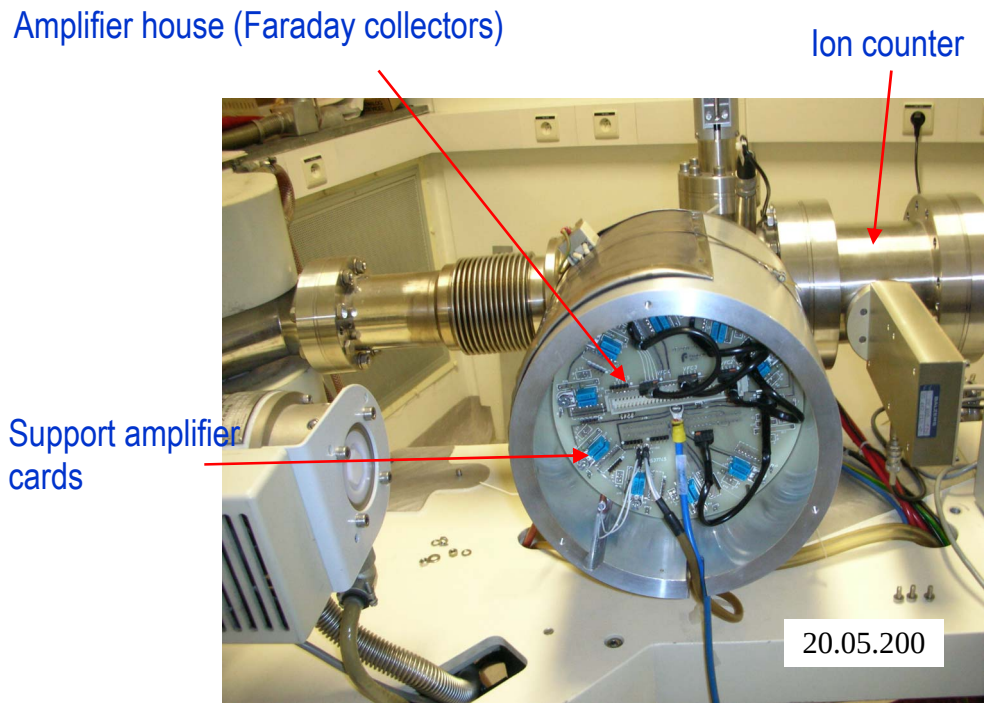

Figure 14: View of the amplifier house for MAT 271, with two Faraday channels

A special remark had to be done relative to the stability of the dynamic calibration factor between the two Faraday channels. In figure 15, the calibration factor for CO_2 isotope amount ratio measurement is shown for a period of fours months. The calibration factor was defined to be calculated by measuring 45 mass-to-charge peak signals on both Faraday channels, time-corrected and applied for all the peak signals acquired on low amplification Faraday channel.

The stability of calibration factor was $4.54*10^{-4}$ for a period of three months, which is significant better than of Faraday-SEM-Ion counter conversion. As this correction is "locally" applied (measured and applied at the same time), this stability has only a meaning as quality check of measurements and doesn't influence directly the uncertainty of the isotope amount ratios.

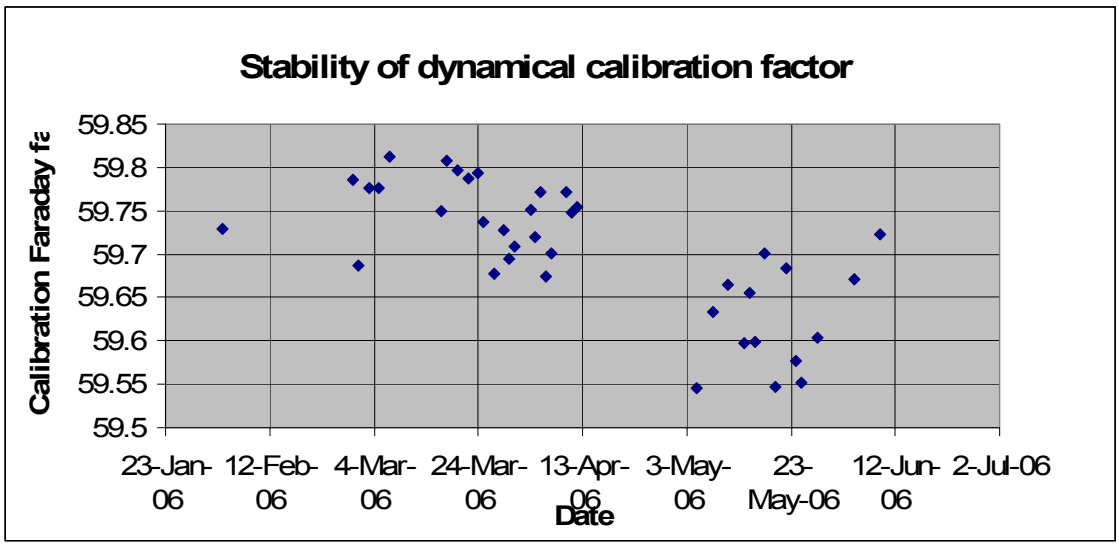

Figure 15: Calibration factor between the two Faraday channels measured and dynamically applied during measurements

3. Measurements and results

A first N_2O sample supplied by Messer company has been measured according to the procedure described above. It must be noticed that a number of nine distinct experiment measurements has been elaborated and performed for defining the complete equation system to be solve for elemental fractional abundances for Nitrogen and Oxygen.

A batch of 200 N_2O bottle produced by Messer company have been bought and few of it have been analyzed using the same method, in order to elaborated a first reference material for Nitrous oxide.

Few details about the results were considered to be of interest to be reported. The first measurement experiment was elaborated for molecular peak signals-mass-to-charge signals 44, 45, and 46. In table 2, the main results for this experiment are shown.

Table 2

sample	Leak rate 44	Leak e45	Leak rate 46	^{45}R	dev. ^{45}R	^{46}R	dev. ^{46}R	Ratio 44/12
1	8.9912E-05	7.996E-05	7.902E-05	0.0076934	5.413E-06	0.0021709	1.0045E-06	28.8453
2	8.9563E-05	7.948E-05	7.912E-05	0.0076902	4.875E-06	0.0021721	1.1934E-06	28.9012
3	8.9881E-05	7.96E-05	7.892E-05	0.0076996	6.994E-06	0.002174	1.0785E-06	29.0045
4	9.0047E-05	7.998E-05	7.91E-05	0.0076956	4.923E-06	0.0021719	9.9786E-07	28.9936

The isotope amount ratio 46/44 was corrected for ion-molecule reaction product (NO_2^+) and also additionally, mass-to-charge 12 peak signal was measured and the ratio 44/12 was used to correct for potential CO_2 impurity in the sample. Only to illustrate the measurement sequence, in fig.16 it is shown the logarithmic plot of mass-to-charge peak signal 44 during the gas flow from the inlet system vessel to the ion source. The linear behavior of the logarithm of the signal is according to the expected molecular gas flow through the gold leak.

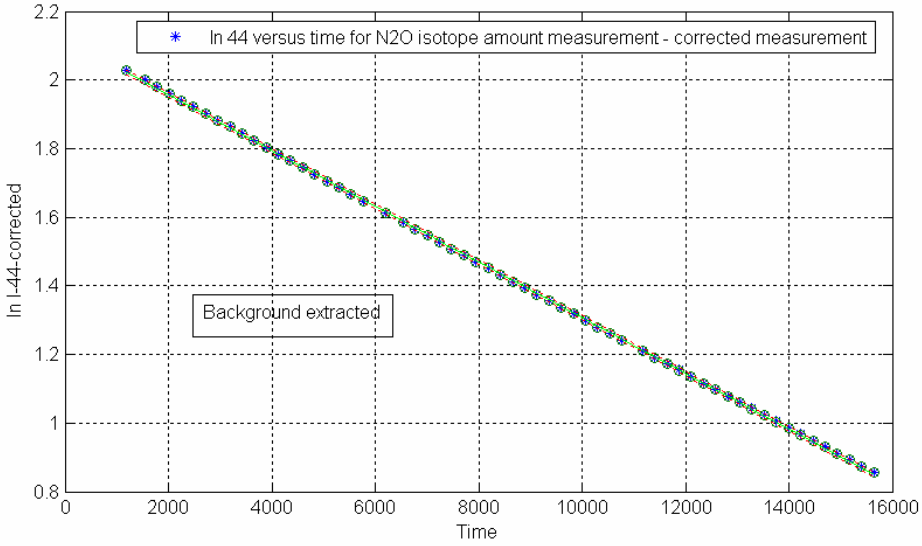

Figure 16: Logarithmic plot of mass-to-charge peak intensity 44 versus time for the main molecular peak measurement experiment for N_2O

A similar plot is also shown in fig.17, for the acquired mass-to-charge signal 45.

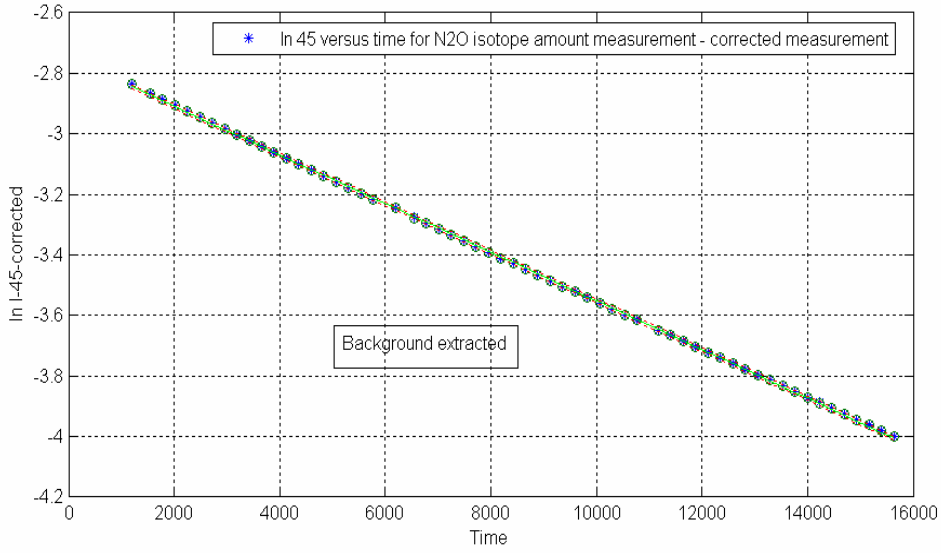

Figure 17.: Logarithmic plot of mass-to-charge peak intensity 45 versus time

However, this is not the case for the acquired 46 mass-to-charge signal. As it was previously mentioned, a significant deviation from the exponential decrease of the 46 peak has been observed due to the production of NO_2^+ ions in the electron impact ion source as a result of the ion-molecule reactions. (fig.18). Therefore, the correction was applied in the way described above, and the NO_2^+ contribution was extracted from the total 46 mass-to-charge signal (fig.19).

After extracting the background contribution to the acquired signals and after applying all the described corrections (CO_2 and NO_2^+ ion-molecule reaction products), the isotope amount ratios 45/44 and 46/44 respectively has been calculated in the time sequence and extrapolated to the t=0, to estimated the original value for the sample (fig.20 and 21)

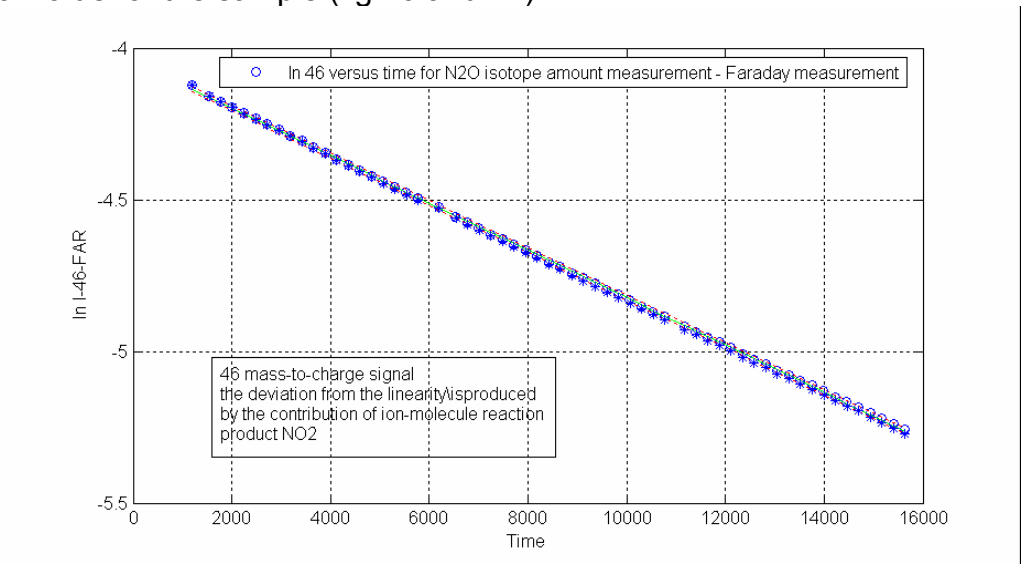

Figure18: Uncorrected acquired 46 mass-to-charge signal for N_2O isotope amount ratio measurement

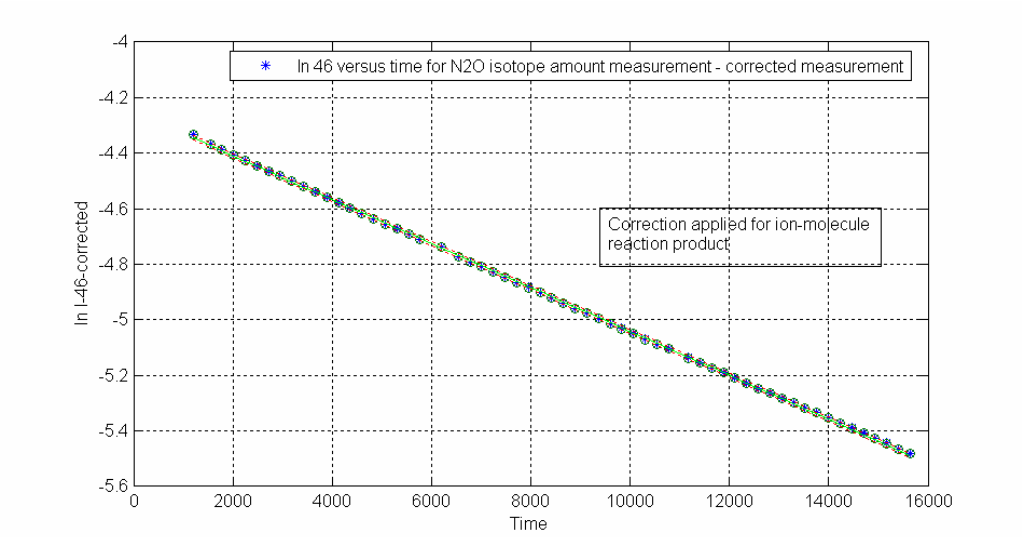

Figure 19: The logarithmic decrease of the 46 mass-to-charge signal after the ion-molecule reaction products NO_2^+ contribution has been extracted

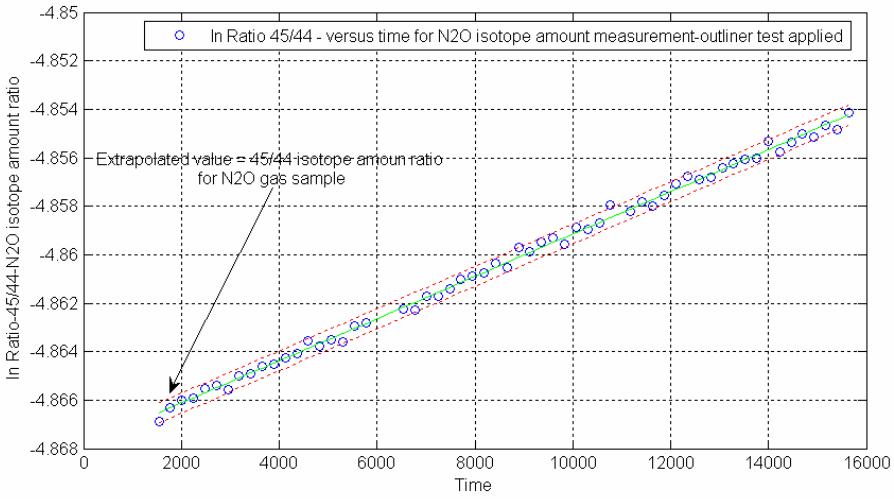

Figure 20: The 45/44 isotope amount ratio for N_2O measurement
The signals are corrected for background and for CO_2 as potential impurities

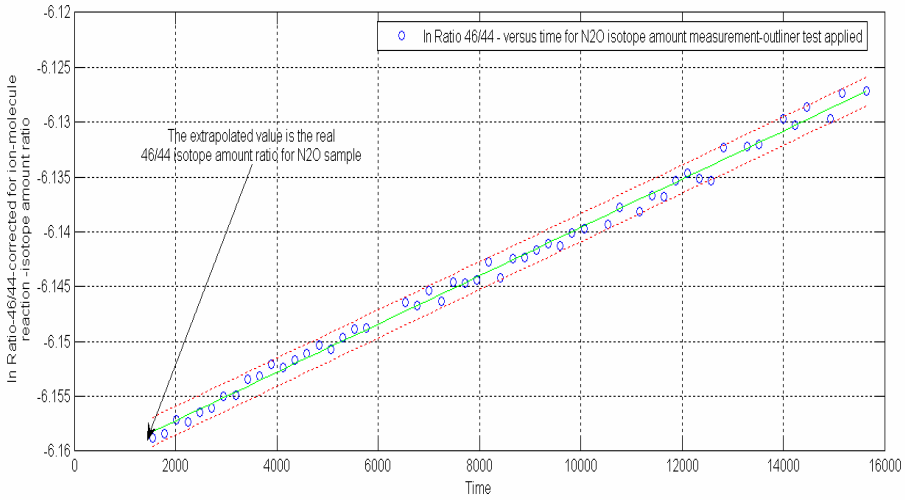

Figure 21: - 46/44 isotope amount ratio for one of the N_2O gas sample
46 mass-to-charge signal has been corrected for NO_2^+ contribution and
44 mass-to-charge signals has been corrected for CO_2 impurity and background

A second set of measurements was done for the NO^+ and N_2^+ fragments by acquiring the mass-to-charge 28(Faraday detector), 29(Faraday detector), 29 (Ion counter), 30(Faraday detector), 31(Faraday detector), 44(Faraday detector) and 12 (Ion counter). The 44 mass-to-charge signal was inserted into the experiment sequence in order to calculate the leak rate 44 – k_{44} and the 12 mass-to-charge signal was used for extracting the CO_2 contribution.

In table 3, there are presented the main results for a set of this type of measurement

Table 3.

No.sample	Leak rate 30	Leak rate 31	Leak rate 32	^{31}R	Std.dev. ^{31}R	^{29}R	Std.dev. ^{29}R
1	5.2942E-05	3.9804E-05	2.4531E-05	0.0074031	3.104E-06	0.00740238	0.00000324
2	5.3451E-05	4.1284E-05	2.6023E-05	0.0074112	2.979E-06	0.00741000	0.00000475
3	5.50674E-05	4.0294E-05	2.7904E-05	0.0074099	4.067E-06	0.00740978	0.00000402
4	5.49023E-05	3.7945E-05	2.8374E-05	0.0074126	3.856E-06	0.00741065	0.00000312

The 31/30 isotope amount ratio plotted against time for one of the measurement done using this experiment is shown in fig. 22.

Finally, a supplementary experiment measurement was performed for determination of 47/46 isotope amount ratio.

The final averaged values for the isotope amount ratios measured on Nitrous oxide sample were shown in table 4.

Table 4

Sample	Ratio 45/44	Std.dev. ^{45}R	Ratio 46/44	Std.dev. ^{46}R	Ratio 47/46	Std.dev. $^{47/46}R$	Ratio 31/30	Std.dev. ^{31}R	Ratio 29/28	Std.dev. ^{29}R
1	7.6917 10^{-3}	2.843 10^{-6}	2.1077 10^{-3}	4.3542 10^{-6}	9.0823 10^{-3}	3.103 10^{-6}	3.991 10^{-3}	1.893 10^{-6}	7.402 10^{-3}	1.673 10^{-6}
2	7.7023 10^{-3}	2.303 10^{-6}	2.1098 10^{-3}	4.023 10^{-6}	9.0992 10^{-3}	3.674 10^{-6}	4.014 10^{-3}	2.783 10^{-6}	7.399 10^{-3}	1.893 10^{-6}
3	7.6852 10^{-3}	3.561 10^{-6}	2.0989 10^{-3}	4.873 10^{-6}	9.1203 10^{-3}	4.142 $10^{=6}$	3.978 10^{-3}	1.956 10^{-6}	7.413 10^{-3}	2.25 10^{-6}
4	7.7045 10^{-3}	4.002 10^{-6}	2.1056 10^{-3}	5.026 10^{-6}	9.0937 10^{-3}	3.892 10^{-6}	3.969 10^{-3}	2.783 10^{-6}	7.387 10^{-3}	2.078 10^{-6}

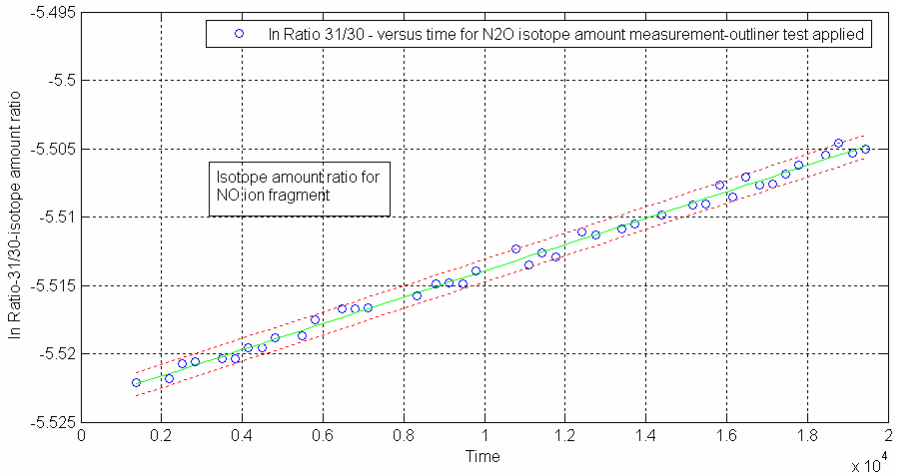

Figure 22: - Isotope amount ratio 31/30 for Nitrous oxide measurement
The extrapolation to t=0 will reveal the original value of this ratio for the investigated sample

Complementary to these isotope amount ratios measurements done for Nitrous oxide gaseous samples, we tried to link these values to the usual Reference material which are used for Nitrogen -Nitrogen Air to express the delta-measurements.

Therefore, a distinct measurement has been elaborated, in a similar manner, for Nitrogen Air, by acquisition of mass-to-charge signals 28 and 29. The acquired signals were prior corrected for CO_2 impurity contribution and for instrumental background and used afterwards to calculate the δ-value for both position-dependent Nitrogen isotope abundances:

$$\delta\left({}^{15}N\right) = \left[\frac{{}^{15}R_{N_2O}}{{}^{15}R_{N_2-air}} - 1\right] \times 1000$$

$$\delta\left({}^{15}N_1\right) = -2.2‰(1.1)$$

$$\delta\left({}^{15}N_2\right) = 12.0‰(1.1)$$

Conclusions

To summarize, a few short conclusions could be drawn from this work:

- ✓ A number of analytical advances were achieved in the isotopic measurement of N_2O including its position-dependent isotope ratios which involved the implementation of the new concept – computer assisted isotopic measurements.
- ✓ A first “absolute” value for position-dependent Nitrogen fractional abundances and Oxygen fractional abundances in Nitrous oxide has been measured and could be released.
- ✓ A first analytical evaluation has been made for the isotopic “scrambling” coefficient.
- ✓ A large field of investigation has been opened relative to the mass-independent isotope fractionation effect for Nitrous oxide. The first tests indicated a relative large deviation from the known exponent value in the Oxygen isotopes relationship.
- ✓ The procedure developed within this work could be successfully applied to other isotopologues measurements. It must be taken into account that the possibility of extracting the contribution of other potential contaminants with the same molar masses is obviously an important achievement of the developed method.
- ✓ δ-value for position-dependent Nitrogen related to Nitrogen-Air Reference material has been measured.

European Commission

EUR 22677 EN – DG Joint Research Centre, Institute for Reference Material and Measurement
Determination by Isotope Ratio Mass Spectrometry of the Absolute Isotope Amount Fractions of Oxygen and Nitrogen in Nitrous Oxide
Authors: VARLAM Mihai, VALKIERS Staf, BERGLUND Michael, TAYLOR Philip

Luxembourg: Office for Official Publications of the European Communities
2007 – 29 pp. – 21 x 29.7 cm
EUR - Scientific and Technical Research series; ISSN 1018-5593
ISBN 978-92-79-03347-6

Abstract

A measurement procedure for the complete isotope characterisation of atmospheric nitrous oxide sample has been developed and applied to establish a first Reference Material for this gas. The whole work has been based on the peculiar instrumental capabilites of "Avogadro" MAT 271IRMS. Additional hardware and software improvement has been done for this mass spectrometer to apply the proposed method .

EUROPEAN COMMISSION
DIRECTORATE-GENERAL
Joint Research Centre

The mission of the JRC is to provide customer-driven scientific and technical support for the conception, development, implementation and monitoring of EU policies. As a service of the European Commission, the JRC functions as a reference centre of science and technology for the Union. Close to the policy-making process, it serves the common interest of the Member States, while being independent of special interests, whether private or national.

LA-NA-22677-EN-C

Publications Office
Publications.eu.int